

## Modulation by PKA of the Hyperpolarization-activated Current ( $I_h$ ) in Cultured Rat Olfactory Receptor Neurons

G. Vargas, M.T. Lucero

Department of Physiology, University of Utah, School of Medicine, 410 Chipeta Way, Salt Lake City, UT 84108-1297, USA

Received: 16 November 2001/Revised: 28 March 2002

**Abstract.** The hyperpolarization-activated  $I_h$  channel is modulated by neurotransmitters acting through the cAMP messenger system. In rat olfactory receptor neurons (ORNs), dopamine, by inhibition of adenylyl cyclase, shifts the voltage of half-maximal activation ( $V_{1/2}$ ) of  $I_h$  to more negative potentials and decreases  $I_h$  maximal relative conductance. Whether these effects result from a phosphorylation-dependent mechanism is unclear. Therefore, we used whole-cell patch-clamp recording techniques to study cAMP-dependent phosphorylation via PKA on  $I_h$  in rat ORNs. General protein kinase inhibition (50 nM K252a) produced a hyperpolarizing shift in  $I_h$   $V_{1/2}$  and decreased  $I_h$  maximal conductance. Specific inhibition of PKA with H-89 (500 nM) also shifted the  $V_{1/2}$  of  $I_h$  to more negative potentials, and, in some cells, decreased  $I_h$  maximal conductance. PKA-mediated phosphorylation (cBIMPS, 50  $\mu$ M) shifted  $I_h$   $V_{1/2}$  more positive, modulated the kinetics of  $I_h$  channel activation and increased  $I_h$  peak current amplitude. Internal perfusion of the catalytic subunit of PKA (84 nM) also shifted  $I_h$   $V_{1/2}$  positive and this shift was blocked by co-perfusion with PKI (50 nM). These results show that in rat ORNs, the voltage dependence of  $I_h$  activation can be modulated by PKA-dependent phosphorylation. We also show that PKA and other protein kinases may be involved in the regulation of  $I_h$  maximal conductance. Our findings suggest that changes in the phosphorylation state of ORNs may affect resting properties as well as modulate odor sensitivity.

**Key words:** Olfaction — Hyperpolarization — Protein kinase A —  $I_h$  — Voltage-gated — Phosphorylation

## Introduction

The hyperpolarization-activated current ( $I_h$ ) is a voltage-gated conductance that was first described as  $I_f$  in the heart (Brown & DiFrancesco, 1980), and as  $I_h$  in central (Halliwell & Adams, 1982; Spain, Schwandt, & Crill, 1987; Pape & McCormick, 1989; Maccaferri et al., 1993) and peripheral neurons (Mayer & Westbrook, 1983; Hestrin, 1987; Pearce & Duchon, 1994; Scroggs et al., 1994), including vertebrate and invertebrate ORNs; (Lynch & Barry, 1991; Corotto & Michel, 1994). The  $I_h$  channel activates upon hyperpolarization of the cell membrane and produces a slowly activating, non-inactivating, inwardly rectifying current. The current is carried by both  $\text{Na}^+$  and  $\text{K}^+$  ions, and under normal physiological conditions has a reversal potential more positive than the resting membrane potential (Mayer & Westbrook, 1983; Spain et al., 1987; McCormick & Pape, 1990). Pharmacologically,  $I_h$  is identified by its sensitivity to external  $\text{Cs}^+$  and relative insensitivity to  $\text{Ba}^{2+}$ , tetrodotoxin, tetraethylammonium (TEA) and 4-aminopyridine (Mayer & Westbrook, 1983; McCormick & Pape, 1990; Lynch & Barry, 1991; Ludwig et al., 1998). Functionally,  $I_h$  plays important roles in the electrophysiological properties of many neurons. When active, it contributes to the resting membrane potential of central and peripheral neurons (Trotier & Doving, 1996; Bal & McCormick, 1997; Lamas, 1998; Wellner-Kienitz & Shams, 1998; Doan & Kunze, 1999), shapes the patterns of neuronal rhythmic firing and controls cell excitability (McCormick & Pape, 1990; Akasu, Shoji, & Hasuo, 1993; Maccaferri & McBain, 1996; Tabata & Ishida, 1996; Wang, Van den Berg, & Ypey, 1997; Hughes, Cope, & Crunelli, 1998; Lüthi, Bal, & McCormick, 1998; Magee, 1998; Wellner-Kienitz & Shams, 1998). In the heart, it plays a key role in cardiac pacemaking activity by the generation and control of diastolic depolarization

and spontaneous firing rate of sinoatrial node cells (Brown & DiFrancesco, 1980; DiFrancesco, Ducoiret, & Robinson, 1989).

Another property of the  $I_h$  channel is its modulation by neurotransmitters and hormones that regulate basal adenylyl cyclase activity and intracellular levels of cAMP ( $[cAMP]_i$ ). Activation of adenylyl cyclase and subsequent increase in  $[cAMP]_i$  result in an enhancement of  $I_h$  due to a depolarizing shift in the voltage dependence of half-activation ( $V_{1/2}$ ) of  $I_h$  (DiFrancesco et al., 1986; Bobker & Williams, 1989; Banks, Pearce, & Smith, 1993; Ingram & Williams, 1996; Larkman & Kelly, 1997), while adenylyl cyclase inhibition and decrease in  $[cAMP]_i$  produce a decrease in  $I_h$  and a hyperpolarizing shift in  $V_{1/2}$  (DiFrancesco & Tromba, 1988; Chang & Cohen, 1992; Pape, 1992; Ingram & Williams, 1994; Vargas & Lucero, 1999b). In bull-frog sympathetic neurons, canine Purkinje fibers and ventricular myocytes, PKA-dependent phosphorylation of the channel underlies the regulation of the voltage dependence of  $I_h$  activation (Tokimasa & Akasu, 1990; Chang et al., 1991; Yu, Chang, & Cohen, 1993, 1995). In addition, cloning of members of the  $I_h$  channel superfamily showed that a PKA consensus phosphorylation site is present in some members of this channel superfamily (Santoro et al., 1998) and that the native channel can exist in a phosphorylated state (Gauss, Seifert, & Kaupp, 1998).

In contrast to the effects of PKA-dependent phosphorylation on  $V_{1/2}$ , of  $I_h$  the effects of phosphorylation on  $I_h$  maximal conductance ( $g_{max}$ ) seem to be more variable. In sympathetic neurons, stimulation of adenylyl cyclase activity enhanced  $I_h$  by increasing its  $g_{max}$  and shifting its  $V_{1/2}$  to more positive potentials; protein kinase inhibition reversed this enhancement of  $I_h$  (Tokimasa & Akasu, 1990). However, in Purkinje fibers,  $I_h$  channel phosphorylation regulated only the  $V_{1/2}$  of  $I_h$  activation; it had no effect on  $g_{max}$  of  $I_h$  (Chang et al., 1991; Yu et al., 1993). In isolated ventricular myocytes,  $I_h$  phosphorylation also produced a positive shift in the  $I_h$  activation curve, but it was not clear whether the conductance was also regulated (Yu et al., 1995). Interestingly, in sinoatrial node cells,  $I_h$  phosphorylation resulted only in an increase in  $g_{max}$  of  $I_h$  (Accili, Redaelli, & DiFrancesco, 1997). Therefore, the regulatory effects of phosphorylation on  $I_h$  seem to vary among different cell types.

In rat ORNs, dopamine modulates  $I_h$  through activation of  $D_2$  dopamine receptors (Vargas & Lucero, 1999b), which results in an inhibition of adenylyl cyclase activity and a decrease in  $[cAMP]_i$  (Mania-Farnell, Farbman & Bruch, 1993; Coronas et al., 1999). Activation of  $D_2$  receptors in rat ORNs produces a hyperpolarizing shift in the  $V_{1/2}$  of  $I_h$  and a decrease in  $I_h$   $g_{max}$ , whereas increasing intracellular cAMP produces a depolarizing shift in the  $V_{1/2}$  (Vargas & Lucero, 1999b). Whether these modula-

tory actions of dopamine on  $I_h$  are due to decreased cAMP alone or result from a reduction in cAMP-dependent phosphorylation (PKA) is still unclear. Therefore, we used whole-cell, voltage-clamp recording techniques to study the modulatory effects of PKA-mediated phosphorylation on the basal properties of  $I_h$  in rat ORNs. We found that PKA regulates the voltage dependence of  $I_h$  activation and, in some cells, the  $I_h$   $g_{max}$ . These results demonstrate that, in rat ORNs,  $I_h$  is modulated by phosphorylation. Since  $I_h$  can contribute to the modulation of cell excitability and to spike frequency adaptation during the excitatory response to odorants (Lynch & Barry, 1991), these findings suggest a mechanism by which dopaminergic regulation of  $[cAMP]_i$  and phosphorylation state in ORNs may set resting properties as well as modulate odor sensitivity.

## Materials and Methods

### CELL PREPARATION AND CULTURE CONDITIONS

Rat ORNs were dissociated and kept in culture as previously described (Vargas & Lucero, 1999a). Briefly, adult male Simonsen albino rats (~200 g) were handled according to the Policy on Humane Care and Use of Laboratory Animals established by the Public Health Service. Rats were deeply anaesthetized (150 mg/kg ketamine + 15 mg/kg rompum, Mallinckrodt Veterinary, Mundelein, IL) and sacrificed by decapitation. The olfactory epithelium from the nasal septum and turbinates of one rat was dissected under 100% oxygen vapor saturated with rat Ringer's, placed in enzyme solution [10 mg/ml bovine serum albumin (BSA), 1 mg/ml collagenase (Gibco BRL; Grand Island, NY), 50  $\mu$ g/ml deoxyribonuclease II and 44 U/ml dispase (Gibco BRL) in divalent cation-free rat Ringer's (in mM: 145 NaCl, 5.6 KCl, 10 Hepes, 10 glucose, 4 EGTA) pH 7.4, 300 mOsm), and incubated with gentle shaking (80 rpm) at 37°C for 45 minutes. Following this incubation period, the tissue was washed with fresh divalent cation-free rat Ringer's, and gently triturated using a fire-polished Pasteur pipette. The resulting cell suspension was filtered, and 200  $\mu$ l were plated onto Concanavalin A (10 mg/ml, Sigma type IV)-coated glass coverslips placed in 35-mm petri dishes. Following a 20-minute settling time, 2 ml of culture medium was added to each dish. The dishes were placed at 37°C in a CO<sub>2</sub> incubator until used (2–4 days). The culture medium [Dulbecco's Modified Eagle Medium (Gibco BRL) supplemented with 100  $\mu$ M ascorbic acid, 1:100 Insulin-Transferrin-Selenium-100  $\times$  (Gibco BRL), 5% fetal bovine serum (Gibco BRL), and 2 mM Glutamine, 100 U/ml Penicillin G, 100 mg/ml Streptomycin (Irvine Scientific; Santa Ana, CA)] was replaced daily. Chemicals were purchased from Sigma (St. Louis, MO) unless stated otherwise.

### ELECTROPHYSIOLOGICAL RECORDINGS

Whole-cell, voltage-clamp recording techniques (Hamill et al., 1981) were performed on rat ORNs kept in culture for up to 4 days. As reported previously (Vargas & Lucero, 1999a, 1999b), no changes in the electrophysiological properties of the cells were observed over time in culture. Electrodes (10–12 M $\Omega$  resistance in 25 mM K<sup>+</sup> rat Ringer's) were pulled from thick-walled (0.64 mm) borosilicate filament glass (Sutter Instrument; San Rafael, CA) on a Flaming/Brown P87 puller. Coverslips with adherent cells were placed into the recording chamber and superfused with the external

bath solution at a rate of 1–2 ml/min. Test solutions were delivered by a multibarrel, rapid solution changer. The external bath solution and the test solutions were maintained at 35°C. The bath solution was grounded with a 3 M KCl agar bridge to a silver chloride wire.

Voltage-clamp experiments were performed as previously described (Vargas & Lucero, 1999b). Briefly, recordings were acquired and digitized using a Digidata 1200 interface, an Axopatch 200A patch-clamp amplifier (Axon Instruments; Foster City, CA), pClamp 5.5 software (Axon Instruments), and a 486-33 IBM clone computer. Data were sampled at 1 kHz and filtered off-line at 500 Hz.  $I_h$  currents were evoked by hyperpolarizing voltage protocols from a holding potential of either  $-40$  or  $-50$  mV. At least three successive voltage protocols were run for each bath solution and averaged. Isolation of the  $I_h$  current component in rat ORNs by subtraction of either the  $\text{Cs}^+$ -insensitive current or the instantaneous current ( $I_{\text{inst}}$ ), has been thoroughly described in our previous work (Vargas & Lucero, 1999b) and was performed in an identical fashion for the present experiments. In addition, as expected for  $I_h$ , the  $\text{Cs}^+$ -sensitive component could be irreversibly blocked by the specific  $I_h$  channel antagonist ZD7288 (100  $\mu\text{M}$ ; gift from Zeneca Pharmaceuticals, *data not shown*). Cells that showed changes in  $I_{\text{inst}}$  over the course of the experiments were not included in the data analyses.  $I_h$  peak current amplitudes were measured at the end of each 3-second hyperpolarizing voltage step. Conductance-voltage ( $g$ - $V$ ) relationships were calculated according to  $g = I/(V - V_r)$ , where  $I$  was the peak current activated at the end of each hyperpolarizing voltage step ( $V$ ), and  $V_r$  was the reversal potential ( $-20 \pm 1$  mV,  $n = 6$ , *data not shown*). The  $g$ - $V$  relationships were fit with a Boltzmann distribution according to  $g = 1/\{1 + \exp[(V_{1/2} - V)/k]\}$ , where  $V_{1/2}$  was the potential of half-maximal activation, and  $k$  was the inverse slope factor. Microcal Origin (Microcal Software; Northampton, MA) and Chanal software (Biodiversity; Park City, UT) were used for data analyses. All averages are reported as mean  $\pm$  standard error of the mean (SEM),  $n$  = number of cells tested for which a complete protocol was obtained.

Passive properties were determined as previously described (Vargas & Lucero, 1999b). Average cell capacitance, membrane input resistance (parallel seal and cell resistance), and uncompensated series resistance were  $4.4 \pm 0.1$  pF,  $1.4 \pm 0.2$  G $\Omega$ , and  $28.1 \pm 0.6$  M $\Omega$  ( $n = 314$ ), respectively. The residual voltage error associated with the remaining series resistance after compensation ranged from 1–3 mV and was not corrected for. The liquid junction potential between the trimethylamine N-oxide (TMA oxide) rat internal solution and the bath solution (25 mM  $\text{K}^+$  rat Ringer's) was 17 mV (calculated using Axoscope, Axon Instruments). The liquid junction potential was subtracted from all records.

## SOLUTIONS

As in our previous studies (Vargas & Lucero, 1999b), the external bath solution used in these experiments was 25-mM  $\text{K}^+$  rat Ringer's in mM: 120 NaCl, 25 KCl, 1 MgCl<sub>2</sub>, 2 CaCl<sub>2</sub>, 10 HEPES, 10 glucose, pH 7.4, 300 mOsm. Previous parallel experiments performed in 2 mM KCl showed similar voltage dependence for  $I_h$ , but reduced current amplitudes (Vargas & Lucero, 1999b). Concentrated stock solutions of K252a (Calbiochem-Novabiochem, La Jolla, CA), H-89 (Calbiochem) and Sp-5,6-DCl-cBIMPS (cBIMPS, BioLog Life Science Institute; La Jolla, CA) were made in DMSO, aliquoted and frozen at  $-20^\circ\text{C}$ . Aliquots were thawed on the day of the experiments and added to the external solution to the desired final concentration.

The internal patch solution used in these experiments was TMA oxide rat internal solution in mM: 62.5 TMA oxide, 62.5 KH<sub>2</sub>PO<sub>4</sub>, 15 KCl, 0.5 CaCl<sub>2</sub>, 2 EGTA, 10 HEPES, 5 MgCl<sub>2</sub>, 2 NaATP, 1 glutathione, 5 TEA, pH 7.2, 310 mOsm. Concentrated stock so-

lutions of the catalytic subunit of PKA (a gift from Dr. Susan Taylor, University of California, San Diego) and PKA peptide inhibitor (PKI, Calbiochem) were made, aliquoted and frozen at  $-80^\circ\text{C}$ . The stock solution of PKA was made in glycerol, while the stock solution of PKI was made in 1 mg/ml BSA solution. Aliquots were thawed on the day of the experiments and added to the internal solution to the desired final concentration. For the PKA and PKI experiments, BSA was also added to the internal solution to a final concentration of 1 mg/ml to prevent loss of enzyme activity (Vargas et al., 1999).

## Results

### PROTEIN KINASE INHIBITORS SHIFT $V_{1/2}$ AND REDUCE $I_h$ $G_{\text{max}}$

In rat ORNs, dopamine, by activation of D<sub>2</sub> receptors, produces a hyperpolarizing shift in the  $V_{1/2}$  of  $I_h$  and a decrease in its  $g_{\text{max}}$  (Vargas & Lucero, 1999b). Activation of dopamine D<sub>2</sub> receptors in ORNs results in an inhibition of adenylyl cyclase activity and a decrease in [cAMP]<sub>i</sub> (Mania-Farnell et al., 1993; Coronas et al., 1999), suggesting that the dopaminergic modulation of  $I_h$  involves the cAMP pathway. The role of a dopamine-induced reduction of PKA-dependent phosphorylation of the  $I_h$  channel remains unclear. To directly study if phosphorylation of the  $I_h$  channel or closely associated proteins modulates the  $V_{1/2}$  of  $I_h$  activation, we tested the effects of protein kinase inhibitors. Figure 1A–B shows an example of the effects of K252a, a non-specific membrane-permeant kinase inhibitor, on  $I_h$  recorded from a cell in the presence and absence of 50 nM K252a.  $I_h$  was activated by a family of hyperpolarizing voltage pulses to  $-140$  mV from a holding potential of  $-50$  mV. Application of 50 nM K252a decreased the amplitude of  $I_h$  as shown in the current-voltage ( $I$ - $V$ ) relationships in Fig. 1A. In this cell, K252a inhibited  $I_h$  at all potentials at which the current was activated. The inhibitory effect of K252a was observed in 9 of 19 cells tested. On average, at a potential of  $-90$  mV, 50 nM K252a produced a  $47 \pm 10\%$  ( $n = 9$ ) reduction of  $I_h$  peak current amplitude. In the 4 cells that survived long enough, the effect of K252a was partially reversed following 10 min of washout, suggesting that the shift was not due to rundown. Current amplitudes were unchanged in the remaining cells.

The reduction of  $I_h$  peak current amplitude can result from a reduced  $g_{\text{max}}$ , a shift in the  $V_{1/2}$ , or both. To determine which parameter K252a modulated, we examined  $I_h$  conductance-voltage ( $g$ - $V$ ) relationships under control conditions and during perfusion of K252a. The conductance at each potential was calculated as described in the experimental procedures, and  $g$ - $V$  relationships were fit with a Boltzmann distribution (smooth lines, Figure 1B). Figure 1B shows the effects of 50 nM K252a on the  $g$ - $V$  relationships for the cell shown in Fig. 1A. The reduction of  $I_h$

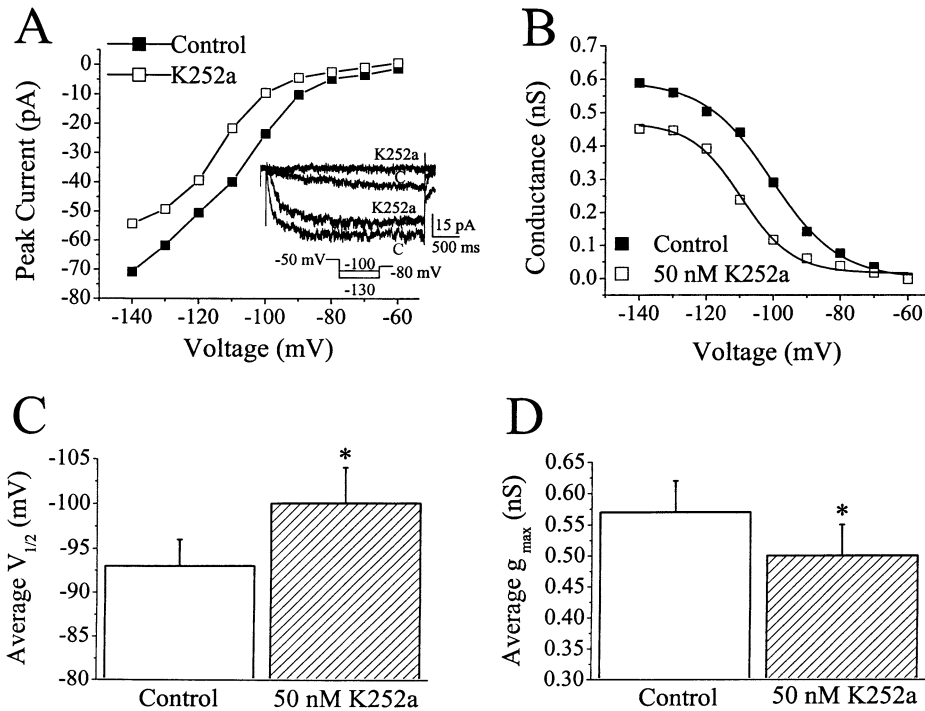


**Fig. 1.** Kinase inhibition decreases  $I_h$  peak currents and maximal conductance and shifts voltage dependence of activation. (A) 50 nM K252a produced a decrease in  $I_h$  current amplitude at all potentials at which  $I_h$  was activated. *Inset:* Cs<sup>+</sup>-subtracted  $I_h$  current traces activated at -100 and -130 mV under control (C) conditions and in 50 nM K252a. (B)  $g$ - $V$  relationships for cell shown in A. The  $V_{1/2}$  and  $k$  under control conditions and in 50 nM K252a were -101 and -9 mV and -109 and -8 mV respectively. The  $g_{max}$  in the absence

and presence of 50 nM K252a was 0.58 nS and 0.46 nS, respectively. (C) The average  $V_{1/2}$  under control conditions and in 50 nM K252a for the cells that responded to application of the kinase inhibitor was  $-93 \pm 3$  mV and  $-100 \pm 4$  mV ( $n = 9$ ) respectively. (D) The average  $g_{max}$  under control conditions and in 50 nM K252a for the cells that responded was  $0.57 \pm 0.05$  nS and  $0.49 \pm 0.05$  nS ( $n = 9$ ) respectively. Asterisks (\*) indicate significance at  $P < 0.05$  using paired Student's  $t$ -test in this and in Figs. 2-4.

current amplitude produced by K252a was a result of both a hyperpolarizing shift in the  $V_{1/2}$  and a decrease in  $I_h$   $g_{max}$ . In this cell, 50 nM K252a produced an 8-mV hyperpolarizing shift in the  $V_{1/2}$  of  $I_h$  activation, and a 21% decrease in  $g_{max}$  (Fig. 1B).

Figure 1C-D shows the effects of K252a on the average  $V_{1/2}$  of  $I_h$  activation and  $g_{max}$ . The hyperpolarizing shift in the  $V_{1/2}$  was observed in all cells that showed a decreased current amplitude with application of K252a ( $n = 9$ ). On average, 50 nM K252a produced a significant  $7 \pm 1$  mV ( $n = 9$ , paired Student's  $t$ -test,  $P < 0.05$ ) hyperpolarizing shift in the  $V_{1/2}$  of  $I_h$  activation (Fig. 1C), with no significant change in the inverse slope factor ( $k$ , average  $k$  under control conditions and in K252a was  $-9 \pm 1$  mV and  $-7 \pm 1$  mV respectively,  $n = 9$ , Student's  $t$ -test,  $P = 0.35$ ), indicating that the sensitivity of  $I_h$  to changes in voltage was unaffected. The decrease in  $g_{max}$  was observed in 7 of the 9 cells that responded to application of K252a, and ranged from 4% to 34% reduction. On average, 50 nM K252a produced a significant  $14 \pm 4\%$  ( $n = 9$ , paired Student's  $t$ -test,  $P < 0.05$ ) reduction of  $I_h$   $g_{max}$  (Fig. 1D).

The results presented in Fig. 1 show that general inhibition of protein kinase activity in rat ORNs re-

sults in a hyperpolarizing shift in the  $V_{1/2}$  of  $I_h$  and a decrease in its  $g_{max}$ . However, from these experiments, it is not apparent which protein kinase is involved in the regulation. To test the involvement of PKA-dependent phosphorylation, we included 1 mM cAMP in the patch-pipette (to activate PKA) and studied the effects of a membrane-permeant PKA-specific inhibitor, H-89 (Chijiwa et al., 1990), on  $I_h$ . As in our previous study (Vargas and Lucero, 1999), cAMP induced a positive shift in the  $V_{1/2}$  ( $n = 6$ ; compare  $V_{1/2}$  of Fig. 1C control+cAMP to Fig. 2C control+cAMP). Four cells tested for H-89 effects did not show a shift in the  $V_{1/2}$  with cAMP in the patch pipette ( $V_{1/2} = -92 \pm 2$  mV) and were not included in further analyses. Figure 2A shows an example of  $I_h$  recorded from a cell in the presence or absence of 500 nM H-89.  $I_h$  was activated by hyperpolarizing voltage steps to -90 and -120 mV from a holding potential of -50 mV. H-89 produced a decrease in the peak current activated at mid-activation potential (-90 mV), but had no effect on the peak current activated at -120 mV (Fig. 2A). In this cell, H-89 produced a 20% reduction in  $I_h$  current amplitude at -90 mV. On average, 500 nM H-89 significantly reduced  $I_h$  current amplitude at -90 mV by  $18 \pm 2\%$  (paired Student's  $t$ -test,  $P < 0.05$ ;  $n = 6$ ).

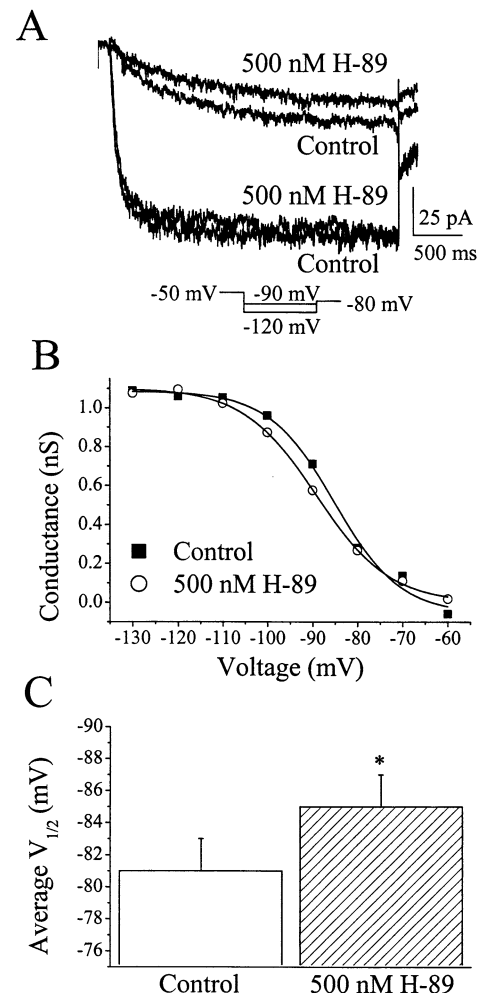


**Fig. 2.** PKA inhibition decreases  $I_h$  peak currents and shifts voltage dependence of activation. In these experiments, 1 mM cAMP was included in the patch pipette. (A)  $\text{Cs}^+$ -subtracted  $I_h$  current traces activated at  $-90$  and  $-120$  mV under control conditions and in 500 nM H-89. The H-89-induced reduction in current amplitude is observed at  $-90$  mV, but not at  $-120$  mV. (B)  $g$ - $V$  relationships for the cell shown in (A). H-89 produced a 4-mV hyperpolarizing shift in the  $V_{1/2}$  with no significant changes in  $k$  and  $g_{\max}$ . (C) The average  $V_{1/2}$  under control conditions and in 500 nM H-89 for the cells that responded to application of the kinase inhibitor was  $-81 \pm 2$  mV and  $-85 \pm 2$  mV ( $n = 6$ ), respectively.

In 2 cells, partial recovery was observed following 10-min washout.

We also examined the effects of H-89 on  $I_h$   $g$ - $V$  relationships. Figure 2B shows the  $g$ - $V$  relationships for the cell shown in Fig. 2A. The  $V_{1/2}$  and  $k$  under control conditions were  $-85$  mV and  $-7$  mV, respectively (Fig. 2B). When H-89 was applied to the cell, the  $V_{1/2}$  and  $k$  were  $-89$  mV and  $-8$  mV, respectively (Fig. 2B). In this cell, H-89 shifted the  $I_h$  activation curve to more negative potentials, with no change in its slope factor. Figure 2C shows the average  $V_{1/2}$  under control conditions and in H-89 ( $n = 6$ ). On average, 500 nM H-89 produced a sig-

nificant  $4 \pm 1$  mV ( $n = 6$ , paired Student's  $t$ -test,  $P < 0.05$ ) hyperpolarizing shift in the  $V_{1/2}$  of  $I_h$  activation with no significant change in  $k$  ( $k$  under control conditions and in H-89 was  $-7 \pm 1$  mV and  $-6 \pm 1$  mV, respectively;  $n = 6$ ,  $P > 0.05$ ).

In the cell shown in Fig. 2A, 500 nM H-89 produced a hyperpolarizing shift in the  $V_{1/2}$  with no change in the  $g_{\max}$  (Fig. 2B). Overall, H-89 had variable effects on the  $g_{\max}$ . In 3 of 6 cells that responded to 500 nM H-89,  $g_{\max}$  decreased by 7 to 18% while in the remaining 3 cells H89 produced no significant changes in  $g_{\max}$ . Therefore, the H-89-induced reduction in  $I_h$  current amplitude results from a negative shift in the activation curve for  $I_h$ , and, in some cells, from a decrease in  $g_{\max}$  also. Together, the results presented in Figs. 1–2 show that in a population of cultured rat ORNs,  $I_h$  is modulated by phosphorylation.

#### PKA MEDIATES REGULATION OF $I_h$

To further examine the role of PKA-dependent phosphorylation on  $I_h$  regulation, we studied the effects of a membrane-permeant PKA activator (cBIMPS) and of adding the catalytic subunit of PKA to the internal solution. Figure 3A shows an example of the effect of cBIMPS on  $I_h$  recorded from one cell superfused with and without 50  $\mu\text{M}$  cBIMPS.  $I_h$  was activated by hyperpolarizing voltage steps to  $-80$  and  $-120$  mV from a holding potential of  $-40$  mV. Perfusion of 50  $\mu\text{M}$  cBIMPS produced an increase in the peak current activated at  $-80$  mV, but had no effect on the peak current activated at  $-120$  mV (Fig. 3). The  $I$ - $V$  relationships for this cell show that 50  $\mu\text{M}$  cBIMPS produced an increase in  $I_h$  current amplitude at mid-activation potentials ( $-80$  to  $-110$  mV), but not at potentials of full activation ( $-120$  to  $-130$  mV, Fig. 3B). In this cell, cBIMPS produced an 83% increase in  $I_h$  peak current activated at  $-90$  mV. On average, at  $-90$  mV, 50  $\mu\text{M}$  cBIMPS produced a significant  $66 \pm 19\%$  ( $n = 7$  of 14 cells tested; paired Student's  $t$ -test,  $P < 0.05$ ) increase in  $I_h$  peak current amplitude. The increase in current amplitude for the cell in Fig. 3A resulted from a 9-mV positive shift in the voltage dependence of  $I_h$  activation with no change in the  $g_{\max}$  ( $g$ - $V$  relationships, Fig. 3C).

Figure 3D shows the effect of 50  $\mu\text{M}$  cBIMPS on the average  $V_{1/2}$  for the cells that responded to application of cBIMPS ( $n = 7$ ). On average, cBIMPS produced a significant  $10 \pm 2$  mV ( $n = 7$ , paired Student's  $t$ -test,  $P < 0.05$ ) depolarizing shift in the  $V_{1/2}$ . Similar to what we observed with H-89, the effect of cBIMPS on  $g_{\max}$  was variable. In 5 of the 7 cells that responded with an increase in current amplitude, 50  $\mu\text{M}$  cBIMPS produced no changes in  $g_{\max}$ . In two cells, however, cBIMPS increased the  $g_{\max}$  by

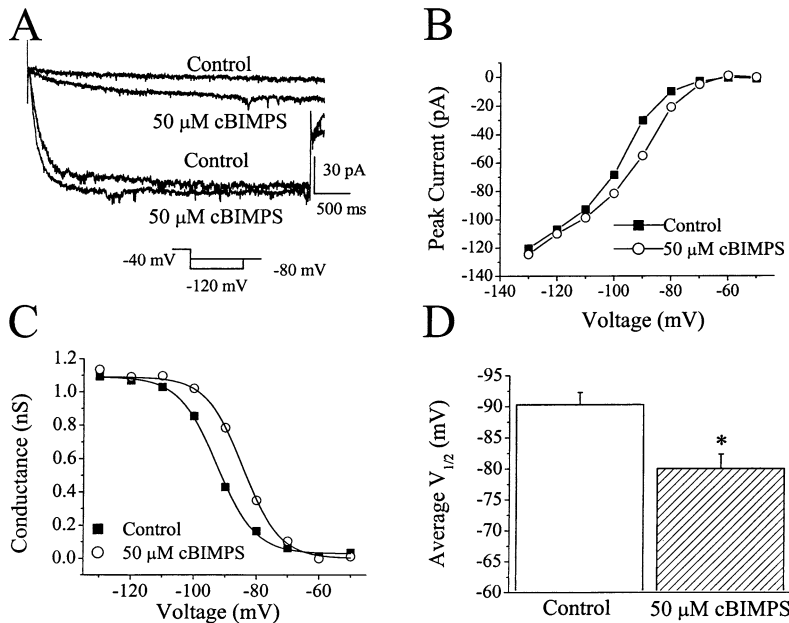


**Fig. 3.** PKA activation increases  $I_h$  peak currents and shifts voltage dependence of activation. (A)  $\text{Cs}^+$ -subtracted  $I_h$  current traces activated by hyperpolarizing voltage pulses to  $-80$  and  $-120$  mV under control conditions and in  $50 \mu\text{M}$  cBIMPS. (B)  $I-V$  relationships for the cell shown in A. (C)  $g-V$  relationships for cell shown in A. The  $V_{1/2}$  and  $k$  under control conditions and in  $50 \mu\text{M}$  cBIMPS were  $-93$  and  $-6$  mV, and  $-84$  and  $-6$  mV, respectively. The  $g_{\text{max}}$  was unchanged. (D) The average  $V_{1/2}$  and  $k$  under control conditions and in  $50 \mu\text{M}$  cBIMPS for the cells that responded to application of this PKA activator ( $n = 7$ ) were  $-90 \pm 2$  mV and  $-8 \pm 1$  mV, and  $-80 \pm 2$  mV and  $-7 \pm 1$  mV respectively.  $50 \mu\text{M}$  cBIMPS produced depolarizing shift in  $V_{1/2}$  of  $I_h$  with no significant change in the slope factor.

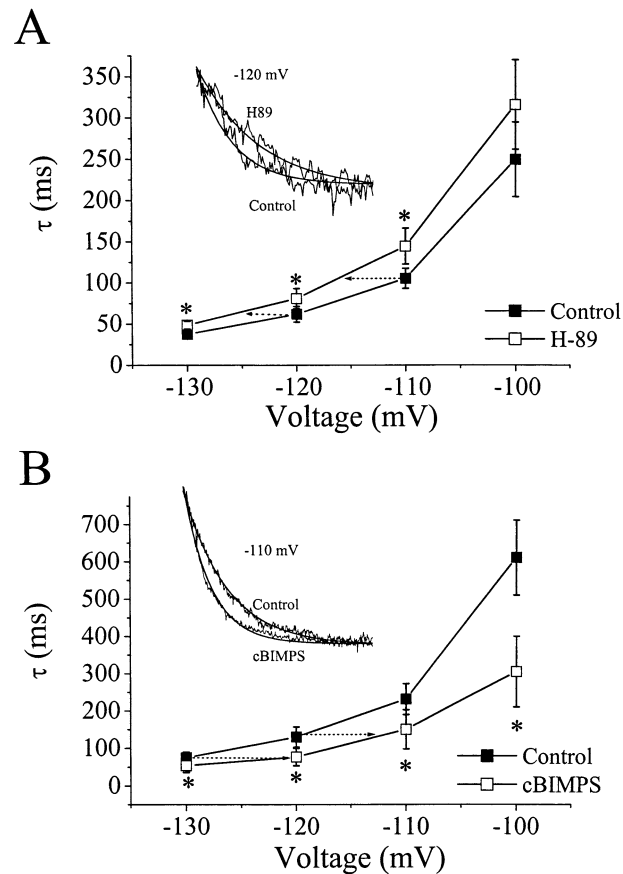
11% and 26% (data not shown). The effects of cBIMPS were not reversed over the 10-min washout period.

The current traces activated at  $-120$  mV under control conditions and in the presence of a PKA activator (cBIMPS, Fig. 3A) suggest that the activation time course of  $I_h$  is faster when the channel is phosphorylated. To investigate if phosphorylation can modulate the kinetics of  $I_h$  activation, we studied the effect of both, H-89 and cBIMPS, on the fast activation time constant ( $\tau$ ) of  $I_h$ . The  $\tau$  was obtained by fitting a single exponential to the initial activation phase of  $I_h$  current traces activated under control conditions and in the presence of either, H-89 or cBIMPS. Figure 4 shows the results obtained; dashed lines and arrowheads indicate the shift in  $\tau$  at these voltages. PKA inhibition ( $500 \text{ nM}$  H-89) significantly slowed the  $\tau$  of  $I_h$  activated at  $-110$  to  $-130$  mV (paired Student's  $t$ -test,  $P < 0.05$ ) and shifted it by  $-5$  to  $-6$  mV (Fig. 4A). Phosphorylation of  $I_h$  had the opposite effect: cBIMPS significantly accelerated the  $\tau$  of  $I_h$  activated at  $-100$  to  $-130$  mV (paired Student's  $t$ -test,  $P < 0.05$ ), and shifted it by  $+8$  to  $+10$  mV (Fig. 4B). These results show that the kinetics of  $I_h$  activation is dependent on the channel's phosphorylation state. The  $I_h$  channel activation is faster when it is phosphorylated (Fig. 4B), while decreased phosphorylation of the channel slows its activation (Fig. 4A).

We also studied the effect of adding the active catalytic subunit of PKA ( $\text{PKA}_c$ ) to the internal solution. Fig. 5A shows the normalized  $g-V$  relationships from four different ORNs. In the control cell, (filled squares) only vehicle ( $1 \text{ mg/ml}$  BSA) was included in the internal patch solution. In a test cell (open triangles)  $84 \text{ nM}$   $\text{PKA}_c$  + BSA was included in

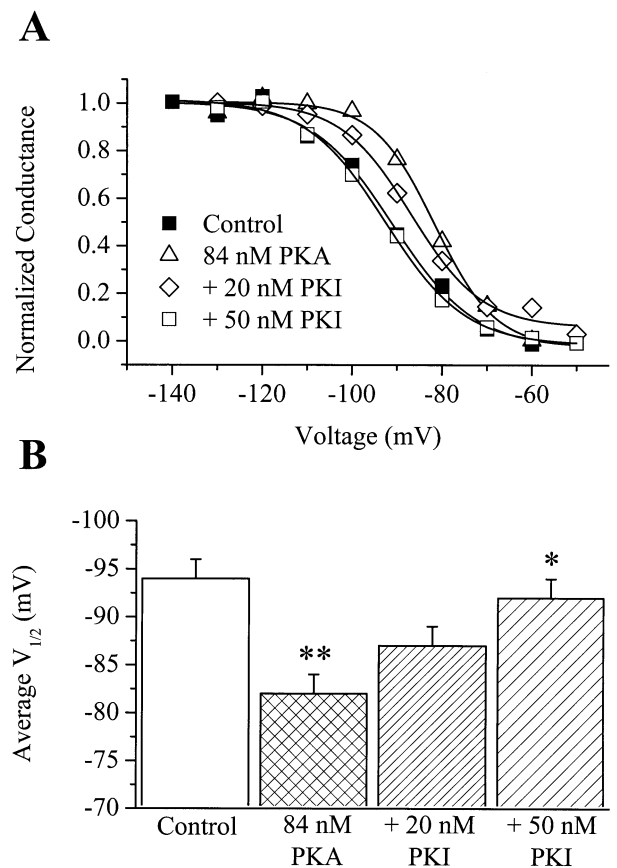
the internal solution. The  $g-V$  relationships for both cells were normalized to their  $g_{\text{max}}$ . The  $V_{1/2}$  and  $k$  for the cell recorded under control conditions were  $-91$  mV and  $-9$  mV, respectively. For the  $\text{PKA}_c$ -dialyzed cell, the  $V_{1/2}$  and  $k$  were  $-82$  mV and  $-7$  mV, respectively. Internal perfusion of  $\text{PKA}_c$  shifted the activation curve of  $I_h$  to more depolarized potentials.

Fig. 5B shows the effect of internal perfusion of  $84 \text{ nM}$   $\text{PKA}_c$  on the average  $V_{1/2}$ .  $I_h$  was recorded from 15  $\text{PKA}_c$ -dialyzed cells and from 15 cells under control conditions. The average  $V_{1/2}$  and  $k$  under control conditions were  $-94 \pm 2$  mV and  $-9 \pm 1$  mV ( $n = 15$ ), respectively. For the cells internally perfused with  $\text{PKA}_c$ , the average  $V_{1/2}$  and  $k$  were  $-82 \pm 2$  mV and  $-9 \pm 1$  mV ( $n = 15$ ), respectively. Internal perfusion of  $84 \text{ nM}$   $\text{PKA}_c$  produced a significant  $12 \pm 2$  mV positive shift in the activation curve of  $I_h$  (one-way ANOVA, Dunnett's Multiple Comparisons post-test,  $P < 0.01$ ) with no significant change in  $k$ . Because the internal perfusion of  $\text{PKA}_c$  was so rapid, we were not able to compare the effect of  $\text{PKA}_c$  on  $I_h$   $g_{\text{max}}$  in the same cell. An unpaired statistical analysis of conductance density obtained by dividing the  $g_{\text{max}}$  by the cell capacitance did not reveal a significant change in  $I_h$   $g_{\text{max}}$  (independent Student's  $t$ -test,  $p = 0.53$ ). The average  $I_h$   $g_{\text{max}}$  density under control conditions and with internal  $\text{PKA}_c$  was  $0.14 \pm 0.01 \text{ nS/pF}$  ( $n = 15$ ) and  $0.12 \pm 0.01 \text{ nS/pF}$  ( $n = 15$ ), respectively. The effects of  $\text{PKA}_c$  on  $I_h$   $V_{1/2}$  were blocked by concurrent application of the PKA peptide inhibitor, PKI. Fig. 5A shows the  $g-V$  relationships for two different cells recorded with internal perfusion of either  $20 \text{ nM}$  or  $50 \text{ nM}$  PKI, in addition to  $84 \text{ nM}$   $\text{PKA}_c$  + BSA. The  $g-V$  relationships were normalized to their  $g_{\text{max}}$ . The  $V_{1/2}$  and



**Fig. 4.** Phosphorylation modulates  $I_h$  channel kinetics. The activation phase of  $I_h$  current traces recorded from cells that responded to either, H-89 ( $n = 6$ ) or cBIMPS ( $n = 7$ ) were fit with a single exponential to obtain the  $\tau$  of activation under control conditions and in the presence of the PKA inhibitor or activator (see insets). (A) Effect of 500 nM H-89 on time constants of  $I_h$  activation. H-89 significantly slowed the activation of  $I_h$  at  $-110$  to  $-130$  mV. (B) Effect of 50  $\mu$ M cBIMPS on time constants of  $I_h$  activation. The activation of  $I_h$  at  $-100$  to  $-130$  mV was significantly faster in the presence of cBIMPS.

$k$  for the cell dialyzed with PKA<sub>c</sub> plus 20 nM PKI were  $-87$  mV and  $-8$  mV, respectively. For the cell dialyzed with PKA<sub>c</sub> plus 50 nM PKI, the  $V_{1/2}$  and  $k$  were  $-93$  mV and  $-9$  mV, respectively (Fig. 5A). On average, internal perfusion of 20 nM PKI produced a  $5 \pm 2$  mV ( $n = 15$ ) hyperpolarizing shift in the  $V_{1/2}$  of  $I_h$ , when compared with 84 nM PKA<sub>c</sub> alone (Fig. 5B). The higher concentration (50 nM) of PKI hyperpolarized the  $I_h$  activation curve by  $10 \pm 2$  mV ( $n = 15$ ) and returned the  $V_{1/2}$  back to control levels (Fig. 5A, B). These results indicate that the effects observed with internal perfusion of the catalytic subunit of PKA were the result of PKA-mediated phosphorylation of the  $I_h$  channel. However, we cannot rule out the possibility that PKA phosphorylated an unknown protein that either increased cAMP levels or interacted with  $I_h$  channels.



**Fig. 5.** PKA modulates the activation curve of  $I_h$ . (A)  $g$ - $V$  relationships for four different cells recorded under four different conditions: control, 84 nM PKA, 84 nM PKA + 20 nM PKI, and 84 nM PKA + 50 nM PKI. Internal perfusion of PKA shifted the  $I_h$  activation curve to more depolarized potentials. PKI blocked the effect of PKA on  $I_h$  in a dose-dependent manner. (B) The average  $V_{1/2}$  and  $k$  ( $n = 15$  for each condition) under control conditions, with 84 nM PKA, with PKA + 20 nM PKI, and with PKA + 50 nM PKI were  $-94 \pm 2$  mV and  $-9 \pm 1$  mV,  $-82 \pm 2$  mV and  $-9 \pm 1$  mV,  $-87 \pm 2$  mV and  $-8 \pm 2$  mV, and  $-92 \pm 2$  mV and  $-9 \pm 1$  mV, respectively. The data was analyzed with a one-way ANOVA with Dunnett's post test using GraphPad Prism version 3.02, San Diego California. Double asterisks (\*\*) indicate groups significantly different from the control group at  $P < 0.01$ ; asterisk (\*) indicates groups significantly different from the PKA (but not from control group) at  $P < 0.05$ .

## Discussion

### EFFECT OF PROTEIN PHOSPHORYLATION ON $I_h$

Protein phosphorylation is a major mechanism involved in the modulation of ion channel properties and function. Phosphorylation of specific residues of the ion channel protein usually leads to altered channel availability or voltage dependence in the membrane electric field, as has been described for  $\text{Ca}^{2+}$  and  $\text{K}^+$  channels (Tsien, Giles, & Greengard, 1972; Reuter et al., 1982; Tsien et al., 1986; Walsh, Begenisich, & Kass, 1988; Trautwein & Hescheler,

1990). Experiments in myocytes using calyculin A, a potent phosphoprotein phosphatase inhibitor, to unmask basal phosphorylation of the  $I_h$  channel established that  $I_h$  is also regulated by protein phosphorylation (Yu et al., 1993, 1995; Accili et al., 1997). These experiments, however, did not determine the protein kinase involved in  $I_h$  channel phosphorylation. Since cAMP acts as the second messenger in the modulation of  $I_h$ , PKA is a likely candidate. Our present study investigated the effects of PKA on  $I_h$  in rat ORNs. The results presented here provide one of the most detailed investigations on the effects of PKA-mediated phosphorylation on  $I_h$  channel properties.

Protein phosphorylation regulates the voltage dependence of  $I_h$  activation. In Purkinje fibers and isolated ventricular myocytes, treatment with calyculin A resulted in a positive shift in the activation curve of  $I_h$  (Yu et al., 1993, 1995). Protein kinase inhibitors produced the opposite effect; in Purkinje fibers, the protein kinase inhibitors H-7 and H-8 shifted the activation curve of  $I_h$  to more negative potentials (Chang et al., 1991). In agreement with these previous observations, we observed a hyperpolarizing shift in the  $V_{1/2}$  of  $I_h$  in ORNs during perfusion of protein kinase inhibitors (Figs. 1, 2). This effect was due in part to inhibition of PKA activity, since H-89, a PKA-specific inhibitor, had an effect similar to, although smaller than K252a, a nonspecific kinase inhibitor. In addition, activation of PKA with cBIMPS (Fig. 3) or internal perfusion of the catalytic subunit of PKA right-shifted the activation curve of  $I_h$ , and the specific PKA peptide inhibitor PKI blocked this effect (Fig. 5). We observed hyperpolarizing shifts in  $I_h$   $V_{1/2}$  with protein kinase inhibitors in 15 of 29 cells even in the absence of adenylyl cyclase stimulation or cAMP perfusion. This finding suggests that, in unstimulated cultured rat ORNs, about half of  $I_h$  channels exist in a phosphorylated state, as has been described for some members of the  $I_h$  channel superfamily (Gauss et al., 1998). Our results also suggest that the basal phosphorylation state of the channel determines the starting position of the  $I_h$  activation curve along the voltage axis. Our observation that roughly half of the cells tested with kinase inhibitors showed no response may reflect the metabolic state of these primary cultures. Cells in culture are in various phases of maturation and apoptosis. We visually selected healthy looking cells, but the lack of effect by either kinase inhibitors or activators may reflect compromised machinery in those cells. The more robust shifts in  $V_{1/2}$  in response to cBIMPS or PKA<sub>c</sub> support the idea that the basal phosphorylation state is relatively low.

In addition to the effect on the voltage dependence of activation, we observed a change in the kinetics of  $I_h$  activation in response to channel phosphorylation. When the channel is in a phosphorylated state (cBIMPS), it activates faster; when

phosphorylation is reduced (H-89), it activates more slowly (Fig. 4). Because  $I_h$  activation kinetics are dependent on voltage (Lynch & Barry, 1991), the shift in the  $V_{1/2}$  of activation due to  $I_h$  phosphorylation ( $4 \pm 1$  mV with H-89 and  $10 \pm 2$  mV with cBIMPS) accounts for the changes in the  $\tau$  of  $I_h$  activation ( $4$  to  $6$  mV with H-89 and  $8$  to  $10$  mV with cBIMPS, Fig. 4). The  $\tau$  measured in rat ORNs was in the range of 100 to 200 msec and is in a similar range as the cloned and expressed HCN1 channel, but an order of magnitude faster than the HCN2 channel (Santoro et al., 1998).

The effects of protein phosphorylation on  $I_h$   $g_{max}$  have not been as carefully studied as the effects on  $V_{1/2}$ . In sinoatrial node myocytes, calyculin A increased  $I_h$   $g_{max}$  without significantly affecting the position on the activation curve of  $I_h$  (Accili et al., 1997). In isolated ventricular and Purkinje myocytes, it was not clear whether phosphorylation modulated  $I_h$   $g_{max}$ , because complete activation curves were not generated due to the very negative position of the activation curve of  $I_h$  in that preparation (Yu et al., 1995). In rat ORNs, we observed a significant decrease in  $I_h$   $g_{max}$  with the general kinase inhibitor K252a. Likewise, inhibition of PKA activity with H-89 decreased  $I_h$   $g_{max}$  in 3 of 6 cells. Internal perfusion of the catalytic subunit of PKA produced no significant changes in  $I_h$  maximal conductance density. This may be explained by the inability to measure  $I_h$   $g_{max}$  before PKA perfused into the cells. The results obtained with H-89 and cBIMPS argue for a role for PKA-dependent phosphorylation in the regulation of  $I_h$   $g_{max}$ . We cannot exclude, however, the involvement of other kinases, such as PKC or tyrosine kinases (Cathala & Paupardin-Tritsch, 1997; Wu & Cohen, 1997), in the modulation of  $I_h$   $g_{max}$ , since general inhibition of kinase activity (K252a) was more effective in reducing  $g_{max}$  than was specific PKA inhibition.

#### PHYSIOLOGICAL SIGNIFICANCE

Our experiments clearly show that  $I_h$  is modulated in rat ORNs by PKA-dependent phosphorylation. ORNs are very small ( $5$ – $7$   $\mu\text{m}$ ) primary sensory neurons with extremely high input resistances [calculated to be  $20$ – $30$  G $\Omega$  (Lynch & Barry, 1989)], so that small currents have large effects on the membrane potential. Although it is not possible to accurately measure resting potentials in such small cells, it is estimated that the resting potential in ORNs is very negative [ $-90$  mV; (Barry & Lynch, 1991; Qu et al., 2000)]. In previous work, we showed that blocking  $I_h$  at potentials near rest could cause a  $14$ -mV membrane hyperpolarization (Vargas & Lucero, 1999b). The small amplitudes and negative voltage range of the  $I_h$  currents in ORNs ( $V_{1/2} = -94$  mV in control and  $-82$  mV with internally dialyzed PKA<sub>c</sub>) are well suited



to their role in modulating the resting properties and excitability near the resting membrane potential.

In vertebrates, olfactory signal transduction is mediated by second messenger cascades initiated by the binding of odorants to members of the odorant receptor family (Buck & Axel, 1991; Breer, Raming, & Krieger, 1994; Shepherd, 1994). The interaction between an odorant and an odorant receptor leads to activation of an olfactory adenylyl cyclase (Pace et al., 1985; Sklar, Anholt, & Snyder, 1986; Lowe, Nakamura, & Gold, 1989; Bakalyar & Reed, 1990), rapid increases in  $[cAMP]_i$  (Belluscio et al., 1998) and activation of PKA (Schleicher et al., 1993, Wetzel et al., 2001). Increased cAMP leads to opening of cyclic nucleotide-gated channels, membrane depolarization, and generation of action potentials (Nakamura & Gold, 1987). Odor-activated PKA has been shown to modulate  $Na^{2+}$  and  $Ca^{2+}$  currents in ORNs (Wetzel et al., 2001). If the PKA activated during odor responses has access to  $I_h$  channels, then  $I_h$  activity would be increased and its depolarizing influence could affect the firing rate of ORNs during odor responses.

In rat ORNs, dopamine inhibits  $I_h$  by activation of dopamine  $D_2$  receptors (Vargas & Lucero, 1999b). Dopamine is present in the olfactory mucosa (Kawano & Margolis, 1985) and mucus (Lucero & Squires, 1998), and its concentration in the mucus is increased by trigeminal stimulation (Lucero & Squires, 1998). Activation of dopamine  $D_2$  receptors present in rat ORNs results in an inhibition of adenylyl cyclase activity and a decrease in  $[cAMP]_i$  (Mania-Farnell et al., 1993; Coronas et al., 1999), which will lead to decreases in PKA activity and dephosphorylation of  $I_h$ . Therefore, increases in dopamine concentration will shift the population of  $I_h$  channels towards a dephosphorylated state, in which  $I_h$  current density will be lower and its responsiveness will be below maximum.

Interestingly, all 4  $I_h$  channel genes (Moosmang et al., 1999) as well as  $D_2$  dopamine receptors (Nickell et al., 1991) are expressed in the axon terminals of ORNs. Dopamine released from periglomerular cells onto the olfactory nerve terminals is thought to inhibit synaptic transmission (Hsia, Vincent, & Lledo, 1999; Ennis et al., 2001). The phosphorylation-dependent shifts in  $I_h$   $V_{1/2}$  described in the present studies are a plausible mechanism for the observed  $D_2$ -mediated inhibition of olfactory nerve input to the bulb.

In conclusion, we have demonstrated a PKA-dependent regulation of  $I_h$  in rat ORNs. This phosphorylation-dependent modulation of  $I_h$  may become important when an efficient mode of channel control is required, such as during the excitatory response to odorants or during conditions of increased dopamine levels, to set the excitability state of ORNs and their nerve fibers to similar levels.

We thank Dr. S. Taylor for providing the recombinant catalytic subunit of PKA used in these experiments, Tu Dang for technical assistance, and Drs. W. Michel, C. Hegg, P. Lombardo and M. Sanguinetti for helpful comments on an earlier version of the manuscript. This work was supported by the NIH NIDCD RO1 Grant DC-02994 to M.T. Lucero.

## References

- Accili, E.A., Redaelli, G., DiFrancesco, D. 1997. Differential control of the hyperpolarization-activated current ( $i_f$ ) by cAMP gating and phosphatase inhibition in rabbit sino-atrial node myocytes. *J. Physiol.* **500**:643–651
- Akasu, T., Shoji, S., Hasuo, H. 1993. Inward rectifier and low-threshold calcium currents contributed the spontaneous firing mechanism in neurons of the rat suprachiasmatic nucleus. *Pfluegers Arch.* **425**:109–116
- Bakalyar, H.A., Reed, R.R. 1990. Identification of a specialized adenylyl cyclase that may mediate odorant detection. *Science* **250**:1403–1406
- Bal, T., McCormick, D.A. 1997. Synchronized oscillations in the inferior olive are controlled by the hyperpolarization-activated cation currents  $I_h$ . *J. Neurophysiol.* **77**:3145–3156
- Banks, M.I., Pearce, R.A., Smith, P.M. 1993. Hyperpolarization-activated cation current ( $I_h$ ) in neurons of the medial nucleus of the trapezoid body: voltage-clamp analysis and enhancement by norepinephrine and cAMP suggest a modulatory mechanism in the auditory brain stem. *J. Neurophysiol.* **70**:1420–1432
- Barry, P.H., Lynch, J.W. 1991. Liquid junction potentials and small cell effects in patch-clamp analysis. *J. Membrane Biol.* **121**:101–117
- Belluscio, L., Gold, G.H., Nemes, A., Axel, R. 1998. Mice deficient in  $G_{Olf}$  are anosmic. *Neuron* **20**:69–81
- Bobker, D.H., Williams, J.T. 1989. Serotonin augments the cationic current  $I_h$  in central neurons. *Neuron.* **2**:1535–1540
- Breer, H., Raming, K., Krieger, J. 1994. Signal recognition and transduction in olfactory neurons. *Biochim. Biophys. Acta Mol. Cell Res.* **1224**:277–287
- Brown, H., DiFrancesco, D. 1980. Voltage-clamp investigations of membrane currents underlying pace-maker activity in rabbit sino-atrial node. *J. Physiol.* **308**:331–351
- Cathala, L., Paupardin-Tritsch, D. 1997. Neurotensin inhibition of the hyperpolarization-activated cation current ( $I_h$ ) in rat substantia nigra pars compacta implicates the protein kinase C pathway. *J. Physiol.* **503**:87–97
- Chang, F., Cohen, I.S. 1992. Mechanism of acetylcholine action on pacemaker current ( $i_f$ ) in canine Purkinje fibers. *Pfluegers Arch.* **420**:389–392
- Chang, F., Cohen, I.S., DiFrancesco, D., Rosen, M.R., Tromba, C. 1991. Effects of protein kinase inhibitors on canine purkinje fibre pacemaker depolarization and the pacemaker current,  $i_f$ . *J. Physiol.* **440**:367–384
- Chijiwa, T., Mishima, A., Hagiwara, M., Sano, M., Hayashi, K., Inoue, T., Naito, K., Toshioka, T., Hidaka, H. 1990. Inhibition of forskolin-induced neurite outgrowth and protein phosphorylation by a newly synthesized selective inhibitor of cyclic AMP-dependent protein kinase, N-[2-(p-bromocinnamylamino)ethyl]-5-isoquinolinesulfonamide (H-89), of PC12D pheochromocytoma cells. *J. Biol. Chem.* **265**:5267–5272
- Coronas, V., Krantic, S., Jourdan, F., Moysse, E. 1999. Dopamine receptor coupling to adenylyl cyclase in rat olfactory pathway: a combined pharmacological-radioautographic approach. *Neurosci.* **90**:69–78
- Corotto, F.S., Michel, W.C. 1994. A hyperpolarization-activated cation conductance in lobster olfactory receptor neurons. *J. Neurophysiol.* **72**:360–365

- DiFrancesco, D., Ducouret, P., Robinson, R.B. 1989. Muscarinic modulation of cardiac rate at low acetylcholine concentrations. *Science* **243**:669–671
- DiFrancesco, D., Ferroni, A., Mazzanti, M., Tromba, C. 1986. Properties of the hyperpolarizing-activated current ( $i_f$ ) in cells isolated from the rabbit sino-atrial node. *J. Physiol.* **317**:61–88
- DiFrancesco, D., Tromba, C. 1988. Muscarinic control of the hyperpolarization-activated current ( $i_f$ ) in rabbit sino-atrial node myocytes. *J. Physiol.* **405**:493–510
- Doan, T.N., Kunze, D.L. 1999. Contribution of the hyperpolarization-activated current to the resting membrane potential of rat nodose sensory neurons. *J. Physiol.* **514**:125–138
- Ennis, M., Zhou, F., Ciombor, K., Aroniadou-Anderjaska, V., Hayar, A., Borrelli, E., Zimmer, L., Margolis, F., Shipley, M. 2001. Dopamine D2 receptor-mediated presynaptic inhibition of olfactory nerve terminals. *J. Neurophysiol.* **86**:2986–2997
- Gauss, R., Seifert, R., Kaupp, U.B. 1998. Molecular identification of a hyperpolarization-activated channel in sea urchin sperm. *Nature* **393**:583–587
- Halliwel, J.V., Adams, P.R. 1982. Voltage-clamp analysis of muscarinic excitation in hippocampal neurons. *Brain Res.* **250**:71–92
- Hamill, O.P., Marty, A., Neher, E., Sakmann, B., Sigworth, F.J. 1981. Improved patch clamp techniques for high resolution current recording from cells and cell free patches. *Pfluegers Arch.* **391**:85–100
- Hestrin, S. 1987. The properties and functions of inward rectification in rod photoreceptors of the tiger salamander. *J. Physiol.* **390**:319–333
- Hsia, A.Y., Vincent, J.D., Lledo, P.M. 1999. Dopamine depresses synaptic inputs into the olfactory bulb. *J. Neurophysiol.* **82**:1082–1085
- Hughes, S.W., Cope, D.W., Crunelli, V. 1998. Dynamic clamp study of  $I_h$  modulation of burst firing and d oscillations in thalamocortical neurons *in vitro*. *Neurosci.* **87**:541–550
- Ingram, S.L., Willaims, J.T. 1994. Opioid inhibition of  $I_h$  via adenylyl cyclase. *Neuron* **13**:179–186
- Ingram, S.L., Williams, J.T. 1996. Modulation of the hyperpolarization-activated current ( $I_h$ ) by cyclic nucleotides in guinea-pig primary afferent neurons. *J. Physiol.* **492**:97–106
- Kawano, T., Margolis, F. 1985. Catecholamines in olfactory mucosa decline following superior cervical ganglionectomy. *Chem. Senses* **10**:353–356
- Lamas, J.A. 1998. A hyperpolarization-activated cation current ( $I_h$ ) contributes to resting membrane potential in rat superior cervical sympathetic neurones. *Pfluegers Arch.* **436**:429–435
- Larkman, P.M., Kelly, J.S. 1997. Modulation of  $I_H$  by 5-HT in neonatal rat motoneurons *in vitro*: Mediation through a phosphorylation independent action of cAMP. *Neuropharmacology* **36**:721–733
- Lowe, G., Nakamura, T., Gold, G.H. 1989. Adenylate cyclase mediates olfactory transduction for a wide variety of odorants. *Proc. Natl. Acad. Sci. USA* **86**:5641–5645
- Lucero, M.T., Squires, A. 1998. Catecholamine concentrations in rat nasal mucus are modulated by trigeminal stimulation of the nasal cavity. *Brain Res.* **807**:234–236
- Ludwig, A., Zong, X., Jeglitsch, M., Hofmann, F., Biel, M. 1998. A family of hyperpolarization-activated mammalian cation channels. *Nature* **393**:587–591
- Lüthi, A., Bal, T., McCormick, D.A. 1998. Periodicity of thalamic spindle waves is abolished by ZD7288, a blocker of  $I_h$ . *J. Neurophysiol.* **79**:3284–3289
- Lynch, J.W., Barry, P.H. 1989. Action potentials initiated by single channels opening in a small neuron (rat olfactory receptor). *Biophys. J.* **55**:755–768
- Lynch, J.W., Barry, P.H. 1991. Inward rectification in rat olfactory receptor neurons. *Proc. R. Soc. Lond. [Biol.]* **243**:149–153
- Maccaferri, G., Mangoni, M., Lazzari, A., DiFrancesco, D. 1993. Properties of the hyperpolarization-activated current in rat hippocampal CA1 pyramidal cells. *J. Neurophysiol.* **69**:2129–2136
- Maccaferri, G., McBain, C.J. 1996. The hyperpolarization-activated current ( $I_h$ ) and its contribution to pacemaker activity in rat CA1 hippocampal stratum oriens-alveus interneurons. *J. Physiol.* **497**:119–130
- Magee, J.C. 1998. Dendritic hyperpolarization-activated currents modify the integrative properties of hippocampal CA1 pyramidal neurons. *J. Neurosci.* **18**:7613–7624
- Mania-Farnell, B.L., Farbman, A.I., Bruch, R.C. 1993. Bromocriptine, a dopamine D2 receptor agonist, inhibits adenylyl cyclase activity in rat olfactory epithelium. *Neurosci.* **57**:173–180
- Mayer, M.L., Westbrook, G.L. 1983. A voltage-clamp analysis of inward (anomalous) rectification in mouse spinal sensory ganglion neurones. *J. Physiol.* **340**:19–45
- McCormick, D.A., Pape, H.C. 1990. Properties of a hyperpolarization-activated cation current and its role in rhythmic oscillation in thalamic relay neurones. *J. Physiol.* **431**:291–318
- Moosmang, S., Biel, M., Hofmann, F., Ludwig, A. 1999. Differential distribution of four hyperpolarization-activated cation channels in mouse brain. *Biol. Chem. Hoppe Seyler* **380**:975–980
- Nakamura, T., Gold, G.H. 1987. A cyclic nucleotide-gated conductance in olfactory receptor cilia. *Nature* **325**:442–444
- Nickell, W.T., Norman, A.B., Wyatt, L.M., Shipley, M.T. 1991. Olfactory bulb DA receptors may be located on terminals of the olfactory nerve. *Neuroreport* **2**:9–12
- Pace, U., Hanski, E., Salomon, Y., Lancet, D. 1985. Odorant-sensitive adenylyl cyclase may mediate olfactory reception. *Nature* **316**:255–258
- Pape, H.-C. 1992. Adenosine promotes burst activity in guinea-pig geniculocortical neurons through two different ionic mechanisms. *J. Physiol.* **447**:729–753
- Pape, H.C., McCormick, D.A. 1989. Noradrenaline and serotonin selectively modulate thalamic burst firing by enhancing a hyperpolarization-activated cation current. *Nature* **340**:715–718
- Pearce, R.J., Duchon, M.R. 1994. Differential expression of membrane currents in dissociated mouse primary sensory neurons. *Neurosci.* **63**:1041–1056
- Qu, W., Moorhouse, A.J., Rajendra, S., Barry, P.H. 2000. Very negative potential for half-inactivation of, and effects of anions on, voltage-dependent sodium currents in acutely isolated rat olfactory receptor neurons. *J. Membrane Biol.* **175**:123–138.
- Reuter, H., Stevens, C.F., Tsien, R.W., Yellen, G. 1982. Properties of single calcium channels in cardiac cell culture. *Nature* **297**:501–504
- Santoro, B., Liu, D.T., Yao, H., Bartsch, D., Kandel, E.R., Siegelbaum, S.A., Tibbs, G.R. 1998. Identification of a gene encoding a hyperpolarization-activated pacemaker channel of brain. *Cell* **93**:717–729
- Schleicher, S., Boekhoff, I., Arriza, J., Lefkowitz, R.J., Breer, H. 1993. A b-adrenergic receptor kinase-like enzyme is involved in olfactory signal termination. *Proc. Natl. Acad. Sci. USA* **90**:1420–1424
- Scroggs, R.S., Todorovic, S.M., Anderson, E.G., Fox, A.P. 1994. Variation of  $I_H$ ,  $I_R$ , and  $I_{LEAK}$  between acutely isolated adult rat dorsal root ganglion neurons of different size. *J. Neurophysiol.* **71**:271–279
- Shepherd, G.M. 1994. Discrimination of molecular signals by the olfactory receptor neuron. *Neuron* **13**:771–790
- Sklar, P.B., Anholt, R.R., Snyder, S.H. 1986. The odorant sensitive adenylyl cyclase of olfactory receptor cells. Differential stimulation by distinct classes of odorants. *J. Biol. Chem.* **261**:15538–15543

- Spain, W.J., Schwandt, P.C., Grill, W.E. 1987. Anomalous rectification in neurons from cat sensorimotor cortex *in vitro*. *J. Neurophysiol.* **57**:1555–1576
- Tabata, T., Ishida, T.A. 1996. Transient and sustained depolarization of retinal ganglion cells by  $I_h$ . *J. Neurophysiol.* **75**:1932–1943
- Tokimasa, T., Akasu, T. 1990. Cyclic AMP regulates an inward rectifying sodium-potassium current in dissociated bull-frog sympathetic neurons. *J. Physiol.* **420**:409–429
- Trautwein, W., Hescheler, J. 1990. Regulation of cardiac L-type calcium current by phosphorylation and G-proteins. *Annu. Rev. Physiol.* **52**:257–274
- Trotier, D., Doving, K.B. 1996. Inward rectifying current  $I_h$  activated by hyperpolarization in frog vomeronasal receptor cells. *Prim. Sensory Neuron* **1**:245–261
- Tsien, R.W., Bean, B.P., Hess, P., Lansman, J.B., Nilius, B., Nozicky, M.C. 1986. Mechanisms of calcium channel modulation by *b*-adrenergic agents and dihydropyridine calcium agonists. *J. Mol. Cell. Cardiol.* **18**:691–710
- Tsien, R.W., Giles, W.R., Greengard, P. 1972. Cyclic AMP mediates the effects of adrenaline on cardiac Purkinje fibres. *Nature* **240**:181–183
- Vargas, G., Lucero, M.T. 1999a. A method for maintaining odor-responsive adult rat olfactory receptor neurons in short-term culture. *Chem. Senses* **24**:211–216
- Vargas, G., Lucero, M.T. 1999b. Dopamine modulates inwardly rectifying hyperpolarization-activated current ( $I_h$ ) in cultured rat olfactory receptor neurons. *J. Neurophysiol.* **81**:149–158
- Vargas, G., Yeh, T.-Y.J., Blumenthal, D.K., Lucero, M.T. 1999. Common components of patch-clamp internal recording solutions can significantly affect protein kinase A activity. *Brain Res.* **828**:169–173
- Walsh, K.B., Begenisich, T.B., Kass, R.S. 1988.  $\beta$ -Adrenergic modulation in the heart. Independent regulation of K and Ca channel. *Pfluegers Arch.* **411**:232–234
- Wang, Z., Van den Berg, R.J., Ypey, D.L. 1997. Hyperpolarization-activated currents in the growth cone and soma of neonatal rat dorsal root ganglion neurons in culture. *J. Neurophysiol.* **78**:177–186
- Wellner-Kienitz, M.C., Shams, H. 1998. Hyperpolarization-activated inward currents contribute to spontaneous electrical activity and  $\text{CO}_2/\text{H}^+$  sensitivity of cultivated neurons of fetal rat medulla. *Neurosci.* **87**:109–121
- Wetzel C.H., Spehr, M., Hatt H. 2001. Phosphorylation of voltage-gated ion channels in rat olfactory receptor neurons. *Eur. J. Neurosci.* **14**:1056–1064
- Wu, J.-Y., Cohen, I.S. 1997. Tyrosine kinase inhibition reduces  $i_f$  in rabbit A sinoatrial node myocytes. *Pfluegers Arch.* **434**:509–514
- Yu, H., Chang, F., Cohen, I.S. 1993. Phosphatase inhibition by calyculin A increases  $i_f$  in canine Purkinje fibers and myocytes. *Pfluegers Arch.* **422**:614–616
- Yu, H., Chang, F., Cohen, I.S. 1995. Pacemaker current  $i_f$  in adult canine cardiac ventricular myocytes. *J. Physiol.* **485**:469–483